T. Stephens, D.C. Johnson, and M.T. Languirand

Beam Path Conditioning for High-Power Laser Systems

Heating of mirrors and windows by high-power radiation from a laser transmitter produces turbulent density gradients in the gas near the optical surfaces. If the gradients are left uncontrolled, the resulting phase errors reduce the intensity on the target and degrade the signal returned to a receiver. Beam path conditioning maximizes the efficiency of the optical system by alleviating thermal turbulence within the beam path.

Optical systems that combine high-power lasers with large-aperture beam directors have been developed as prototypes for a number of tactical defensive weapon systems, and have been proposed for large-scale strategic defense systems. Several such systems are currently in use for propagation measurements and for long-range high-resolution imaging radar applications. For efficient operation, advanced systems use adaptive optics techniques to control the wavefront phase distribution [1]. The controller measures and corrects the wavefront irregularities introduced by the laser device and internal optical train imperfections between the laser and the exit aperture of the beam director. The controller must also provide corrections for the unavoidable aberrations in the external propagation path caused by natural atmospheric turbulence and the lensing (or *thermal blooming*) caused by absorption of the transmitted beam in the atmosphere. While the controller is designed to correct wavefront distortions, in practice thermal turbulence created by heated laser optics can overwhelm the ability of the controller to correct the external disturbances [2].

Optical distortion created by uncontrolled air temperature gradients is a problem that is not confined to high-power laser systems. The mirrors and supporting structure in astronomical telescopes typically cool more slowly than the nighttime air. The resulting temperature offsets create thermal turbulence, or mirror currents, that can seriously degrade performance [3]. One solution commonly used by astronomers is to open the dome and let the ambient winds carry the thermal currents out of the beam path. This approach is not practical in high-energy beam directors because the temperature gradients are greater than those found in astronomical telescopes and because the system is confined in a tubular shield to contain scattered laser energy.

Wavefront errors can result from thermoelastic distortions of discrete optical elements such as mirrors and solid windows, and from inhomogeneities in the gaseous medium within the beam path. Laser-heated mirrors, windows, and beam ducts transfer heat to the nearby gas and produce perturbations in the refractive index. The gas is also directly heated by absorption of the laser beam. Suppression of these perturbations depends upon active control of the environment in the beam path and typically requires either evacuation of the path or controlled flows of conditioned gas. The flow must be strong enough to provide the needed sweeping or mixing, but not so fast as to introduce appreciable density variation or acoustic noise, or cause vibrations of the structure by buffeting. The design of the beam path conditioning system therefore combines aspects of solid mechanics, fluid mechanics, heat transfer, and control systems, coupled with considerations of the optical performance of the system.

The design, hardware, and performance verification of flowing-gas beam path conditioning systems is complicated and costly. Integration of the conditioning system with the usual elements of a high-power optical train requires close coordination of the engineering efforts. Compromises that accommodate all the required features are inevitable in both the conditioning system design and the optical layout.

Upgrading the scale of conventional flowing-gas designs to systems of much larger size, with shorter operating wavelengths and improved optical performance requirements, promises to be substantially more costly and involve greater risks.

Figure 1 is a photograph of the 1.8-m Sealite beam director in a typical configuration. Figure 2 shows a typical arrangement of a high-power laser optical system illuminating a distant target. Because the laser device usually operates in a partial vacuum, it is housed in a pressure-tight enclosure. The beam emerges through a vacuum window in the enclosure, proceeds through an array of bench-mounted optical components that measure and correct errors in the outgoing wavefront, and passes via an extended beam relay path through the base of a gimballed telescope that expands and points the beam to the target. Laser light reflected from the target, or light generated by a beacon near the line of sight to the target, returns through the telescope to the optical bench and a sensor that detects the errors in the returning wavefront. The sensed return-wave errors are nulled by a deformable mirror on the bench; this system maximizes the laser intensity on the target and the power returned to the receiver. The resolution and dynamic range of the wavefront sensor, and the corresponding spacing, stroke, and control bandwidth of the actuators of the deformable mirror, are ideally governed by the

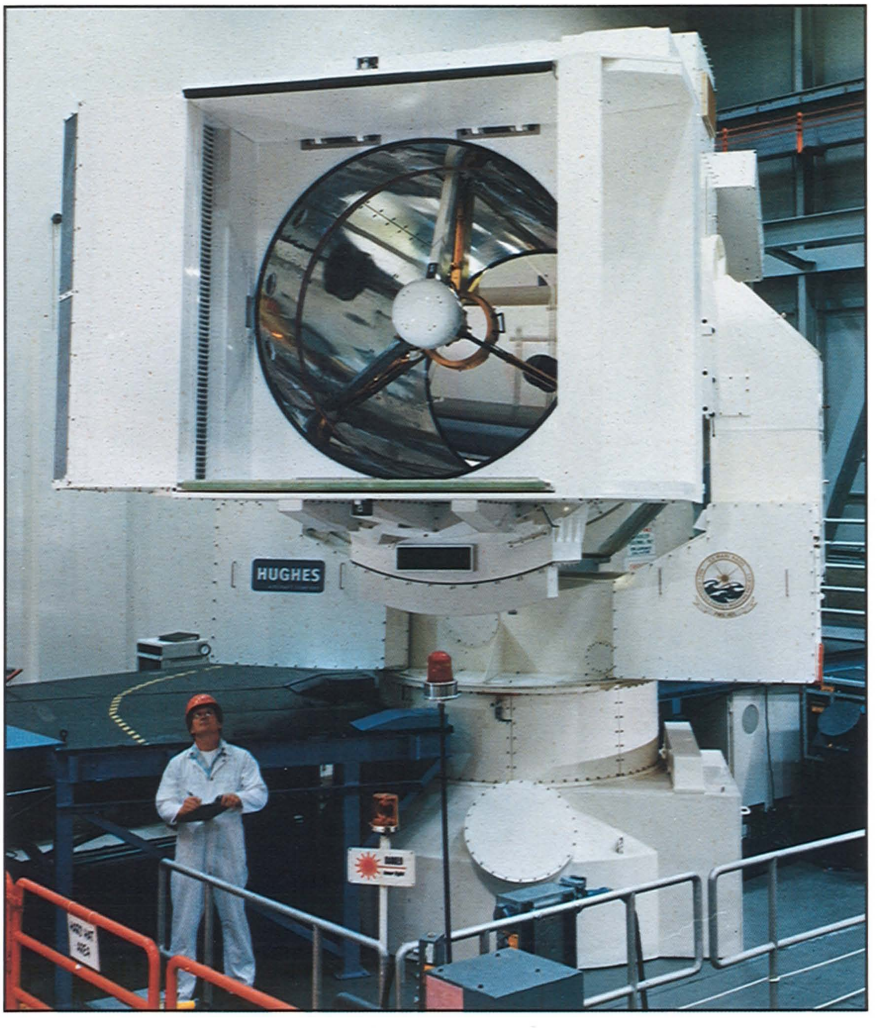

Fig. 1—The 1.8-m-diameter Sealite beam director. This mount is typical for the high-energy laser systems discussed in this article. (Photo courtesy of U.S. Navy.)

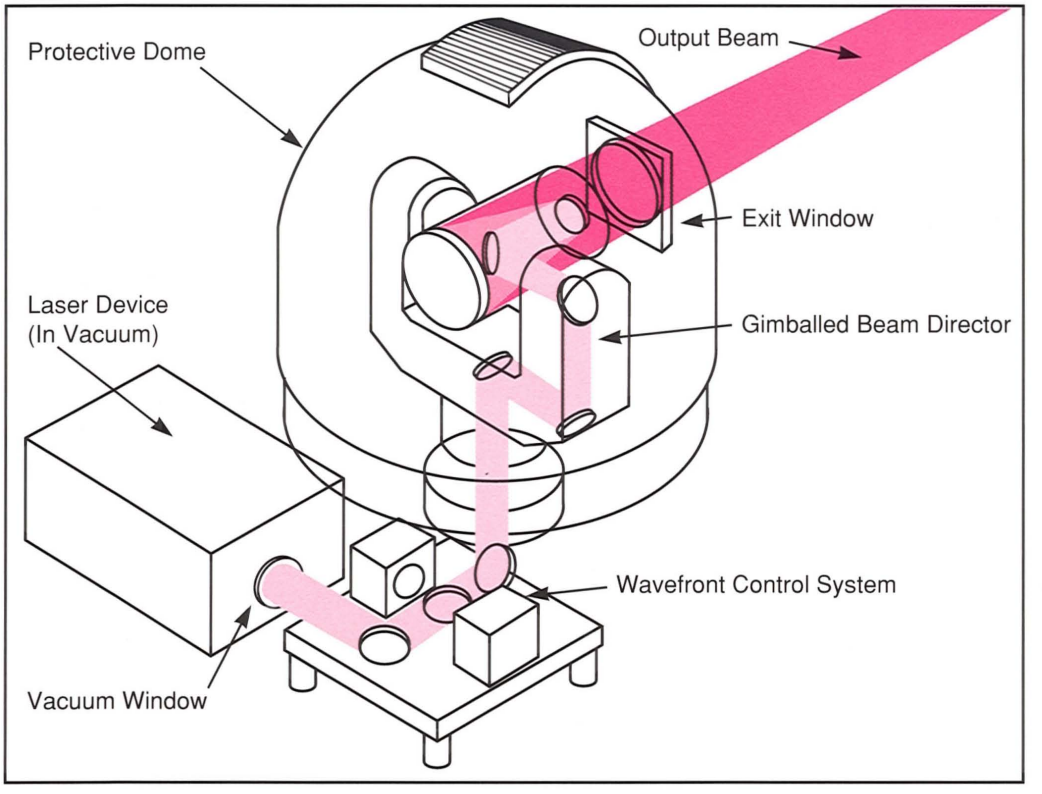

Fig. 2—Ground-based laser beam director. The laser is generated in a vacuum, is passed through a wavefront correction system, and is expanded and pointed by a beam director. Absorption of the laser by the optics creates temperature gradients and results in thermal turbulence, which leads to uncorrectable wavefront errors.

worst operating conditions of thermal turbulence (or *seeing*) that can be anticipated in the external propagation path, with some margin for correction of internally generated phase errors. Typically, these spacings are between 5 to 10 cm (when referred to the exit aperture), the strokes are 5 to 10 μm, and the bandwidths are up to 1 kHz. Phase disturbances outside these limits are uncorrectable and should be avoided.

Aero-Optic Effects

Refractive-index variations in the conditioning gas arise from imperfect mixing of different gases or from density variations in an otherwise homogeneous gas. Density variations result from pressure or temperature gradients. Pressure gradients are typically associated with the forced flow of conditioned gas through the beam path, and the density variation is proportional to the square of the flow speed (for Mach numbers less than 0.3). For example, at standard conditions in air, a speed of 27 m/sec (60 mph) produces a reduction in density equal to that produced by a rise in temperature of 1 K. Temperature gradients are the most common cause of wavefront errors in beam path conditioning systems, and system designers attempt to reduce the gradients that create these phase errors.

The refractive index of gases is typically close to unity, with a small increment above unity proportional to the gas density and weakly dependent on wavelength. The value of this increment for air at 20°C and one atmosphere pressure, and for a wavelength of 1 μm, is 2.8×10^{-4}. At constant pressure, the refractive index of air accordingly decreases by approximately 1 ppm/K. For example, if two light rays pass through air paths each 1 m in length but differing in average temperature by 1 K, the ray traversing the cooler path is retarded by 1 μm relative to the other.

Small residual uncorrected wavefront phase errors result in a reduction in the on-axis intensity relative to the diffraction-limited case (the *Strehl ratio*) by a quantity approximately equal to the illumination-weighted mean-square phase error. For example, a 1-dB (20%) reduction in on-axis intensity results from an rms phase error of 0.45 radians, or $\frac{1}{14}$ wavelength. If this phase error were attributed solely to air heating effects, it would correspond to an uncompensated temperature difference-length product of 0.07 K-m for the entire optical train (for a wavelength of 1 μm). Temperature differences greater than 1 K are expected at several places along the beam path, so the axial extent of the temperature differences must be limited.

Vacuum Windows

For practical convenience, the optical bench and beam director of working systems typically operate at atmospheric pressure, with a controlled flow of conditioned air or a gas mixture that has a refractive index similar to air at the same conditions. This scheme was dictated partly by difficulties in providing economical large vacuum windows capable of reliably transmitting high powers at the transmitter and receiver wavelengths, with acceptably low aberrations.

Aerodynamic Windows

Carbon-dioxide gas dynamic lasers were the first practical devices capable of operating at high power for extended periods. In these devices the pressure in the laser cavity is on the order of $\frac{1}{10}$ atmosphere. Since suitable materials were not immediately available for small solid windows operating at these wavelengths, alternative approaches were developed on the basis of aerodynamic effects.

Figure 3 illustrates a typical aerodynamic window [4] that consists of a jet of air blown at supersonic speed across the aperture in the vacuum enclosure. The pressure difference across the aperture causes the jet to curve

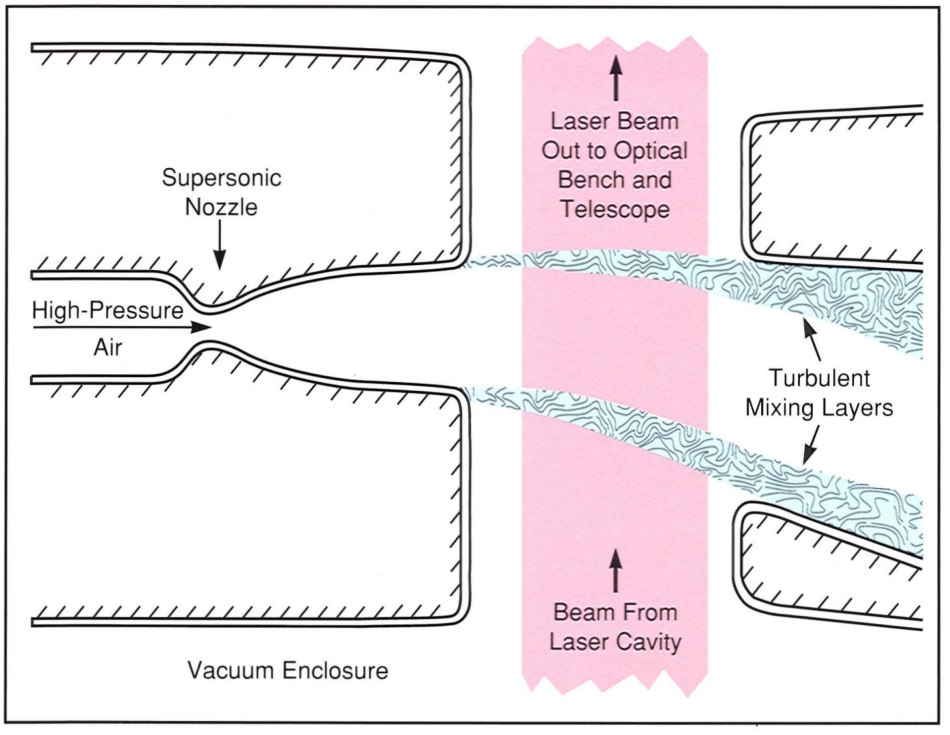

Fig. 3—Schematic drawing of an aerodynamic vacuum window. Vacuum is maintained in the laser cavity by closing the opening with a supersonic jet of air.

toward the evacuated space. With appropriate nozzle design, the flow field within the beam approximates a portion of a linear vortex in which the streamlines curve around a common centerline; the density field depends only on the distance from this centerline. The resulting refractive index field corresponds to a weak diverging cylindrical lens. The jet is captured by a duct and exhausted away from the laser. The jet flow entrains gas from both the high-pressure and low-pressure sides in turbulent mixing layers that thicken as they cross the aperture. Because the turbulence scale and the corresponding length scale and magnitude of the refractive index perturbations increase with the size of the aperture, small apertures are favored. Substantial mass flow and pumping power is required for these windows, but they are relatively robust when compared to solid windows. In many cases these windows are the only feasible approach for small high-power apertures.

Solid Vacuum Windows

As the technology of high-power laser devices has advanced, the supporting technologies have also progressed. Applications that use higher powers, shorter wavelengths, and larger output apertures are now contemplated. For example, the free-electron laser (FEL) offers the promise of high-power operation at wavelengths in the 1-μm range. FELs operate in relatively high vacuum, so aerodynamic windows are less suitable. Glasses of high optical quality and low absorption at these wavelengths are now available in large sizes for use in windows and lenses.

Three basic options exist for the size and location of a solid vacuum window: a full-aperture exit window, a reduced-aperture interface window between the optical bench and beam expander, and a reduced-aperture window at the exit of the laser. The window can be a flat plate or a shallow dome. Glass must have sufficient thickness to withstand the tensile stresses caused by the bending loads (glass, like many brittle materials, is relatively weak in tension). Alternatively, if the mass or absorbed power of the flat plate window is too great, the window can be a shallow spherical shell in which the vacuum load results in a compressive stress in the glass, and the thickness is dictated primarily by elastic stability (or *buckling*) [5]. A familiar example is the faceplate on a television cathode-ray tube. Figure 4 shows the minimum thickness of glass required to withstand a one-atmosphere pressure load over a given diameter. For moderate edge angles, the minimum allowable thickness of a dome is more than an order of magnitude smaller than for a flat plate. However, the cost of machining and optical finishing of large thin spherical windows is greater than that for flat windows of the same size.

Full-Aperture Vacuum Window

The window can be placed at the exit of the telescope so that most of the optical train can be evacuated to a low pressure such that perturbations to the density of the residual gas within the enclosed beam path introduce negligible phase errors (a well-established technique in solar observatories) [6]. This approach eliminates the need for a conventional flowing-gas beam path conditioning system, with the exception of a system to control the thermal boundary layer on

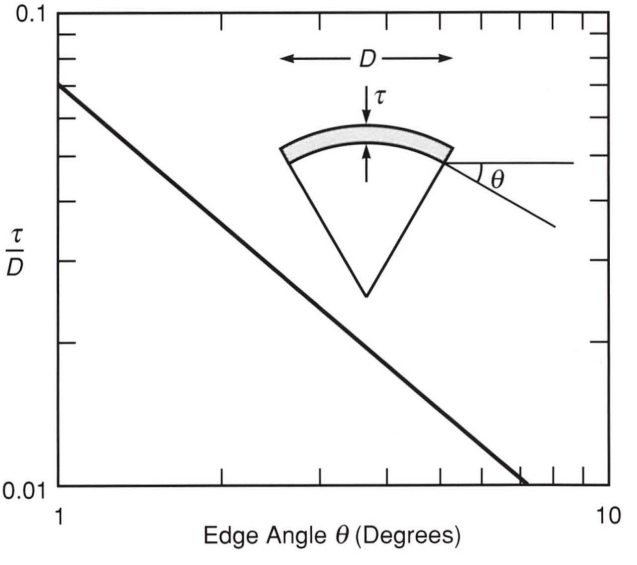

Fig. 4—Solid window thickness as a function of window curvature. Thinner windows result in less absorbed power and smaller wavefront errors.

the outer surface of the exit window. Wind-blown contaminants are physically excluded from the internal optical path. For telescope apertures larger than available glass blanks, solid window segments supported on a structural frame are used [7].

Containing the entire internal propagation path within the vacuum barrier introduces practical problems. Access to the optical components is more restricted, and the forces due to atmospheric pressure transmitted through the barrier can disturb static alignment. Structural failure of the window can result in an implosion and catastrophic damage to the beam director. These concerns need to be addressed in the initial layout, the structural design, and the internal beam alignment system. Further development is necessary to provide confidence in the design of these large windows. For segmented windows, the optical thickness of the segments must be matched to submicron tolerances, which requires advances in the capability of instruments that control the optical finishing process.

Reduced-Aperture Vacuum Window

A full-aperture vacuum window is impractical for larger systems; instead, a reduced-aperture vacuum window can be placed in the unexpanded beam path. The laser intensity in the beam path can be two orders of magnitude greater than at the telescope exit, and it may approach the damage threshold for window surface coatings. Because of heat build-up, active cooling is necessary for extended operating time. Figure 5 shows three basic options that can be considered for this window: (a) an antireflection coated flat at near-normal incidence; (b) an uncoated flat at Brewster's angle; and (c) a coated spherical dome.

A window at Brewster's angle minimizes reflection of the polarization component in which the electric field is parallel to the incidence plane. This window can be applied when the polarization of the laser device is inherently linear, as in an FEL. The use of this window avoids the need for an antireflection coating, and minimization of the fraction of the transmitter power reflected by the window is limited only by the accuracy of the optical

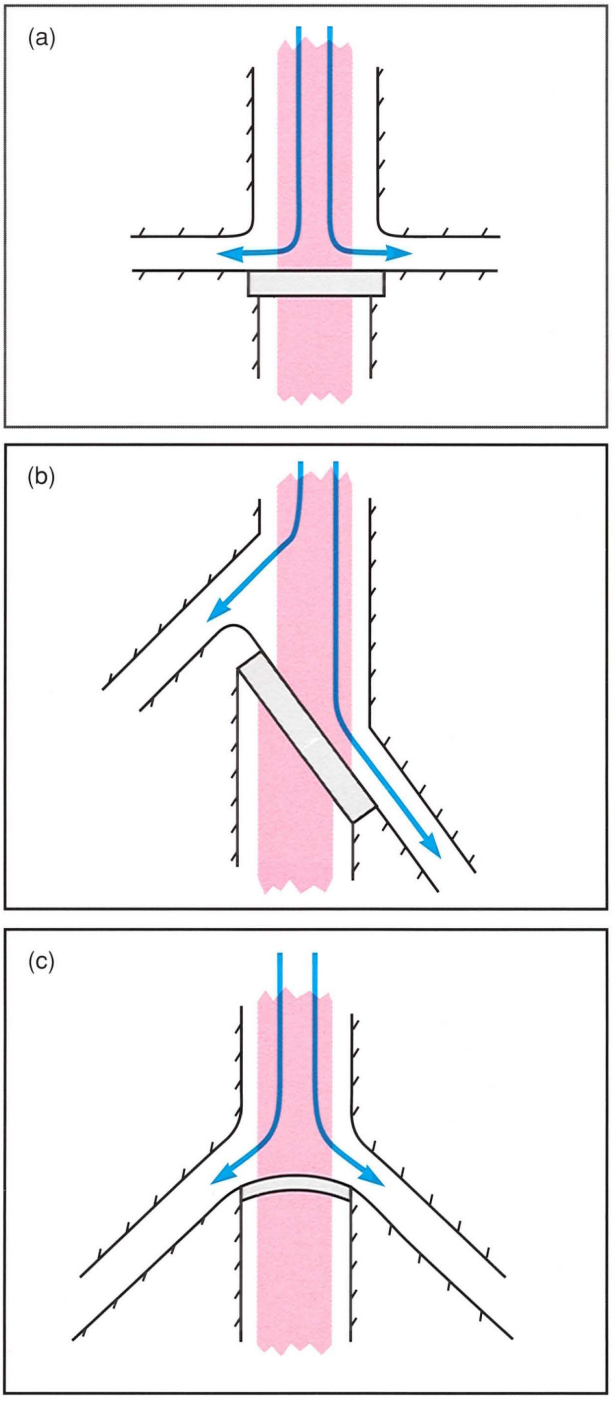

Fig. 5—Vacuum-window designs: (a) near-normal incidence window requires antireflective coatings that may limit peak temperature; (b) Brewster window is thicker than near-normal incidence window but does not require antireflective coatings; (c) spherical-dome window requires antireflective coatings but is thin enough to gain some benefit from active cooling.

finish and mounting angle.

A Brewster window is less suitable for systems in which the transmitter is either unpolarized or the polarization direction is not fixed with respect to the window. In these cases a flat window oriented at near-normal incidence or a spherical dome is more appropriate, but both windows generally require coatings to minimize the reflection loss. The coated surfaces are relatively vulnerable to damage from the transmitted pulses, in comparison to the uncoated surfaces of the Brewster window. The allowable maximum temperature of the coatings are also typically limited to 100°C.

These windows become heated by absorption of the laser beam and cannot be effectively cooled by conduction to the edge. Forced convection of the conditioning gas on the high-pressure side of the window can provide some cooling; forced flow is also necessary to control the refractive-index perturbations in the vicinity of the heated surface.

Thermal Boundary-Layer Control

When a solid surface is at a temperature different from surrounding gas, heat is conducted to (or from) the gas, and a thermal boundary layer develops adjacent to the surface. Buoyancy forces can then cause vertical currents (*free convection*) and formation of plumes of heated (or cooled) gas that extend for appreciable distances away from the surface. In general, the surface temperature differs from that of the ambient gas because of the lag in response to a changing gas temperature or absorption of the transmitted beam.

If the solid surface is a mirror or window in the optical path, then the associated aberrations could become significant if the spatial extent of these heat-driven flows in the direction of optical propagation is not limited. The plumes can be influenced by stray currents, such as drafts through the open port in the outer dome. The extent of the free-convection or wind-driven plumes is curtailed by the superposition of a strong forced flow across the surface of the window or mirror. For example, forced flow can be conveniently induced by the transfer of momentum from a low-volume flow of gas issuing from a set of small nozzles at high speed. The region of temperature mismatch is then confined at the surface to a thin wedge that increases in thickness with distance from the source.

Turbulent Wall Jets

Figure 6 shows one method of controlling the thermal boundary layer on the surface of a centrally obscured optical element such as a telescope exit window or primary mirror. A radially outflowing turbulent surface jet is propelled by high-pressure air flowing from a circular array of closely spaced small outward-pointing nozzles. Nozzle diameters are approximately 0.5 mm, with circumferential spacing on the order of 10 nozzle diameters, and a supply pressure of 3 to 5 atmospheres. The flow at the exit of each nozzle, which is initially supersonic, immediately begins to entrain the ambient gas by turbulent mixing to form a spreading and decelerating jet. These miniature jets merge within a radial distance of approximately 10 nozzle spacings to form a uniform outflowing turbulent *wall jet* that hugs the surface according to a process known as the Coanda effect. Figure 7 shows the time-averaged velocity and temperature distribution for a heated surface within this jet. The characteristic thicknesses of the temperature and velocity profiles increase linearly with distance from the source nozzles, and the peak velocity varies inversely with this distance [8].

The effective extent of the time-averaged perturbation to the optical path induced by the heated air layer is found by integrating the temperature distribution, normalized by the surface temperature rise. The characteristic distance is found to be approximately 0.01 times the radial distance from the source nozzles, and the corresponding area-weighted rms time-averaged distance is 0.0012 times the overall diameter. Because this perturbation component is essentially static and of very low spatial frequency (mainly focus), it is readily correctable. The time-varying perturbation components associated with the turbulence in the jet are less correctable and so are of greater

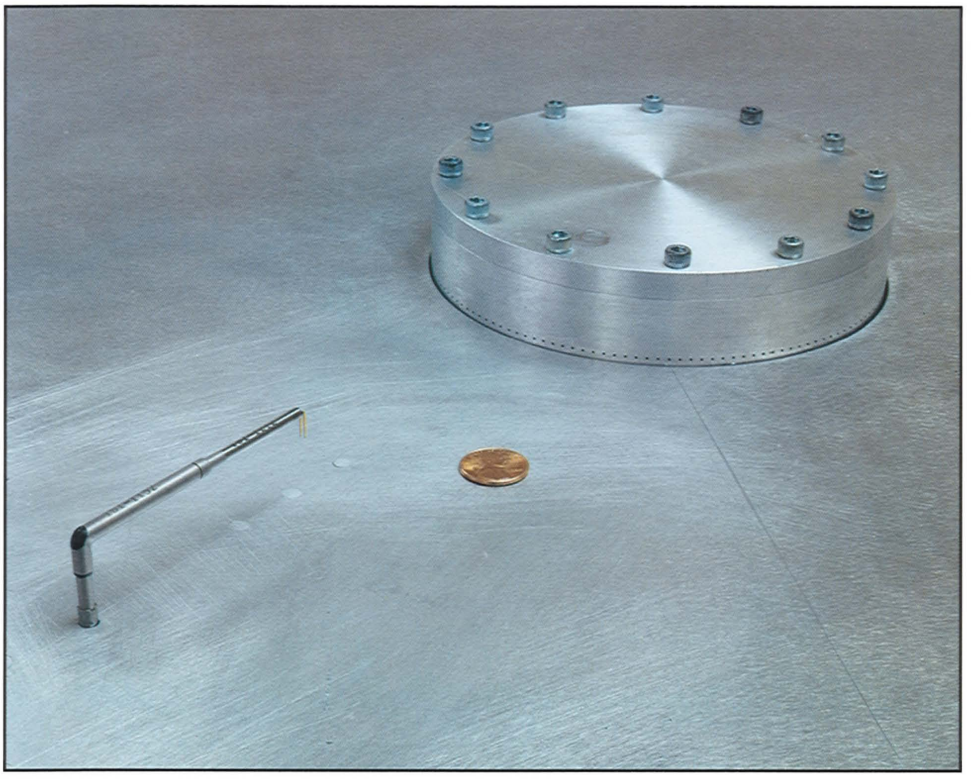

Fig. 6—Radial thermal boundary-layer control jet for centrally obscured optics such as a primary mirror. The jet acts as a momentum pump to create a vigorous flow of cooling gas adjacent to the optic surface. The sensor shown was used to collect temperature and velocity data for the flow.

interest. Time-resolved measurements of the temperature integrated through the jet at a given radial station show a fluctuating component with an rms amplitude approximately one-third of the time-averaged integral. The area-weighted rms value of this fluctuating

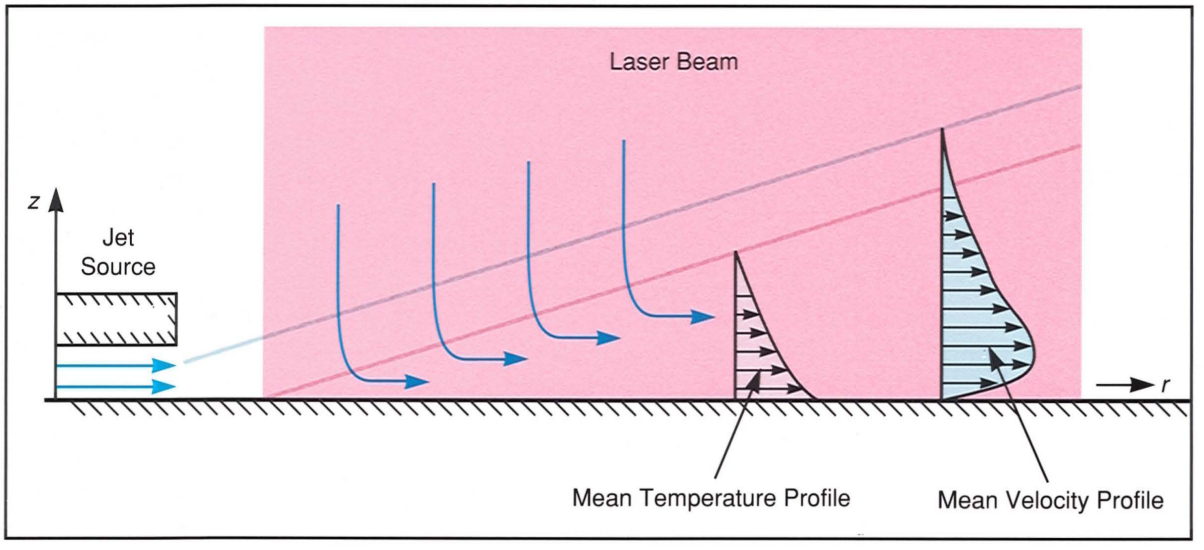

Fig. 7—Schematic drawing of the boundary-layer control jet. The velocity and temperature profiles are governed by viscous shear at the solid surface and turbulent mixing with the quiescent gas. The profile thicknesses increase with distance from the jet source.

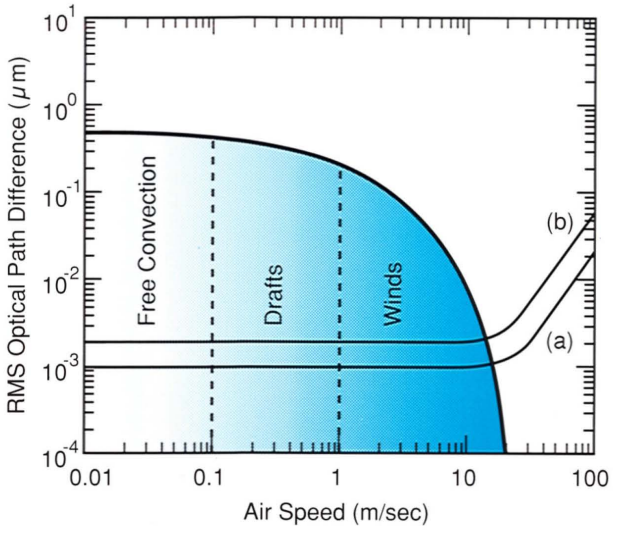

Fig. 8—Variation of rms optical path difference with flow speed for a 1-m-diameter optic with a uniform 1 K temperature rise: (a) radial boundary-layer control jets; (b) transverse boundary-layer control jets. Uncontrolled free convection and ambient winds significantly degrade optical performance. Jets improve performance by controlling thermal turbulence, although performance is limited by compressibility effects at higher velocities. Jet speed is chosen to offset expected draft velocities.

component, normalized by the surface temperature difference, is therefore approximately 0.0008 times the overall diameter. For example, the effect introduces an 0.8-nm rms wavefront distortion in an air jet near the surface of a 1-m-diameter window with a 1 K mismatch in temperature with the ambient air. This distortion is proportional to the diameter and the surface temperature offset.

Turbulent radial wall jets are effective and convenient for centrally obscured solid windows at large apertures. If the window must be placed in the beam path at reduced aperture, however, the central region may not be readily accessible. In this case, a transverse wall jet that spans the entire beam can be used. The scaling laws for jet velocity and jet thickness are different in this case; they result in a slightly larger wavefront distortion for the same aperture diameter and surface temperature offset.

Compressibility Effects

The potential effects of compressibility (i.e., velocity effects) can also be estimated, and the fluctuating component is again of great interest. For example, a radial jet in the center of a 1-m-diameter optic, with a peak velocity of 10 m/sec, produces a fluctuating wavefront distortion of 0.2-nm rms over the 1-m diameter. This amplitude scales linearly with the diameter and with the square of the peak jet velocity at the outer radius. Figure 8 shows the variation of these two wavefront error components with air speed (defined as the peak jet radial velocity at the outer radius), for a nominal diameter of 1 m and a surface temperature offset of 1 K. Because the two effects are generally uncorrelated, the rss determines the total effect. The compressibility effect is not significant for jet speeds below approximately 20 m/sec, compared to the temperature effect at 1 K.

Optimum Flow Speed

The flow speed must be chosen to be greater than that of any disturbing flows at the surface. Figure 8 indicates several regions of disturbance speed. Free-convection flows are typically limited to speeds below 0.1 m/sec, indirect drafts from wind or ventilation flows are expected in the range of 0.1 to 1 m/sec, and direct wind intrusion occurs at speeds up to the operationally allowable maximum of 15 m/sec. If convection currents from the window or mirror are completely uncontrolled (i.e., with zero jet speed), then relatively large wavefront errors can occur. An upper bound can be placed on the estimate of these disturbances. If one side of the beam is filled with air at ambient temperature and the other side contains air at the surface temperature, then the rms temperature difference across the aperture is one-half the surface temperature offset from ambient. If the characteristic length is arbitrarily assumed to be equal to the aperture diameter, then the upper bound on this source of wavefront distortion, as indicated in Fig. 8, is 0.5-μm rms for a 1-m aperture and a 1 K temperature offset in air. These numbers represent a substantial wavefront error in a typical system. The optimum choice of jet speed for typical systems appears to lie in the range from 5 to 30 m/sec,

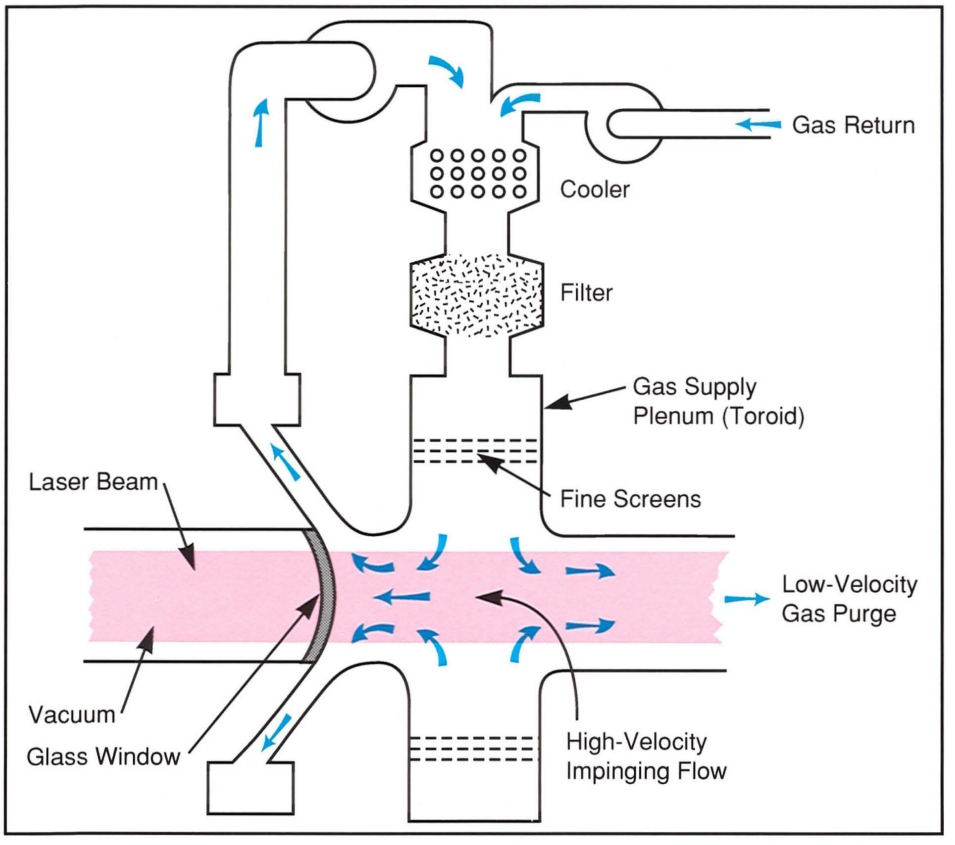

Fig. 9—Schematic drawing of impingement-flow cooling system.

depending on sensitivity to intruding wind flows and cooling requirements.

Impingement Flows

Figure 9 shows an alternative flow arrangement for reduced-aperture solid vacuum windows. In this example, a uniform flow of conditioned air or other gas flows along the beam path, impinges on the window surface, and collects in an annular duct surrounding the window. Thus the thermal boundary layer is swept outward and remains thin and laminar over the surface of the window. The predicted wavefront distortions introduced by the thermal boundary layer in this case are essentially static, with low spatial frequency and with magnitude less than 1 nm.

Cooling Effects

The gas flow that controls the thermal boundary layer on a window or mirror produces a cooling effect sufficient to allow operation for extended or indefinitely long periods. The cooling effect, which is expressed as the *film coefficient* and quantitatively defined as the ratio of heat-transfer rate per unit surface area to the difference between the surface and gas bulk temperatures, depends on the external flow field. Figure 10 compares the film coefficient for the turbulent radial wall jet, the transverse turbulent wall jet, and the axial impingement flow, for a total air flow of $\pi/4$ m^3/sec. (For the turbulent-jet examples, the total flow includes the primary propelling flow and the entrained flow. The entrained flow is typically 20 to 50 times the primary flow.) The film coefficient associated with the radial flow varies inversely with the distance from the central nozzle ring, so it has a pronounced peak near the axis, while the film coefficient associated with the transverse flow varies approximately as the inverse square root of the distance from the source nozzles. In contrast, the film coefficient for the impingement flow is uniform over the aperture but of

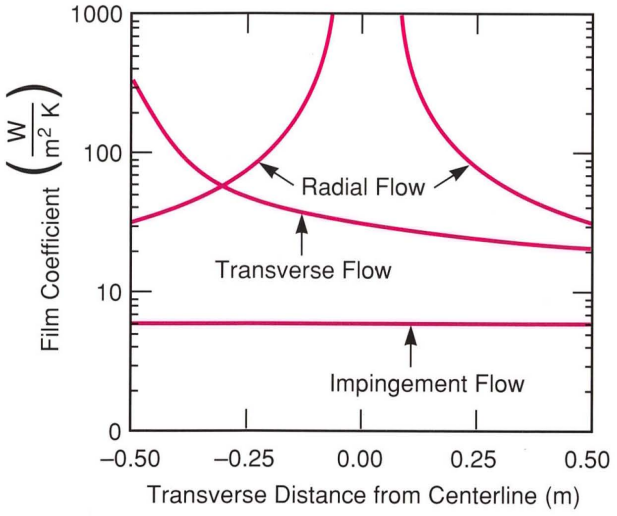

Fig. 10—Relative heat-transfer coefficients for a 1-m-diameter optic with constant total mass flow for a radial boundary-layer control jet, a transverse boundary-layer control jet, and an impingement-flow jet. Radial boundary-layer control jets yield the best heat-transfer performance, but they can be used only on centrally obscured systems.

lower magnitude than the other cases.

Atmospheric Exit Windows

If the vacuum window is located in the reduced-diameter beam path, and the optical train between the vacuum window and the exit aperture of the telescope is maintained at atmospheric pressure with a conditioned gas system, then inevitably mismatches will occur in the refractive index of the conditioned gas relative to the ambient air at the exit of the telescope. Such mismatches can arise from use of a conditioning gas other than air or from temperature differences. A method of minimizing the axial extent (i.e., in the direction of optical propagation) of the zone dividing the two gaseous environments must then be provided.

For example, if the internal path is conditioned with helium at atmospheric pressure and matched in temperature to the outside air, the difference in refractive index between the two environments would be approximately 250 parts per million. Irregularities in the flatness of the surface separating the inner and outer zones would then result in wavefront errors on the order of 0.25 μm per millimeter of axial displacement of this surface. This separation could be implemented with a solid flat exit window, either monolithic or formed from a number of flat segments that have closely matched optical thickness and are supported in a structural frame. Control of the thermal boundary layers on both the inside and outside surfaces would be required, and a system using turbulent radial wall jets would be the natural candidate for a centrally obscured system.

If the internal path is conditioned instead with clean dry air, temperature offsets will be the primary source of wavefront distortion, at approximately 1 μm per meter of axial displacement of the dividing surface, per degree C of temperature offset. If the conditioning gas is allowed to mix with the outside air, then the mixing zone must be limited in axial extent. Wind currents blowing into the telescope could disturb the shape of the zone separating the internal conditioning purge gas from the outside air.

As a worst case, for example, the telescope tube could be filled on one side by conditioning gas and on the other side by ambient air. The resulting effective displacement in the dividing surface would then be approximately equal to the telescope aperture diameter, multiplied by the focal ratio, and further multiplied by the number of axial passes of the beam within the telescope (e.g., three for a Cassegrain telescope). A 1-m-diameter Cassegrain telescope with focal ratio of 1.5 could therefore suffer a worst-case wavefront distortion of 4.5 μm (peak to peak) per degree of temperature mismatch. This value clearly represents a major potential source of wavefront distortion, which would generally require some remedy.

Two basic approaches can be considered as a solution to this wavefront distortion: forced mixing within the telescope, and prevention of wind intrusion. In the first approach, an array of jets stirs the gas mixture within the telescope while the intrusion of outside air is not prevented. This action reduces the size of the inhomogeneities and the amplitude of temperature excursions within the mixture, and results in

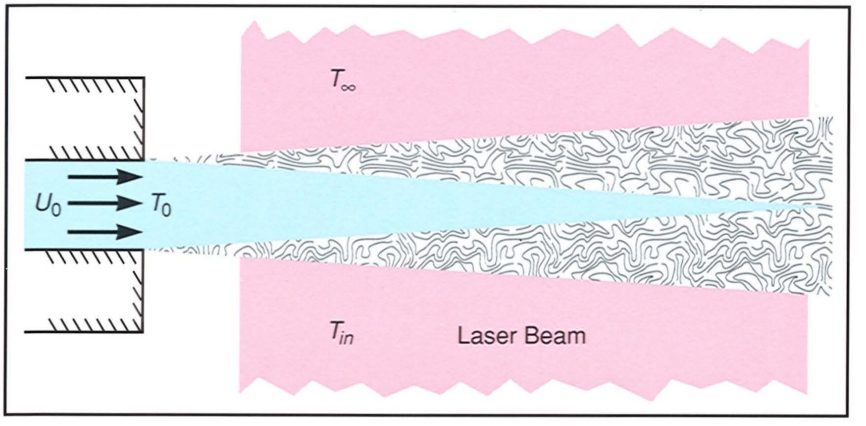

Fig. 11—Single-layer air curtain. The jet at temperature T_0 and velocity U_0 sweeps across the aperture that separates the ambient environment at temperature T_∞ from the beam path conditioning system at temperature T_{in}. Turbulent mixing of the jet and quiescent air creates high spatial-frequency wavefront errors. Ideally, $T_0 = T_{in}$, which leaves only one thermally turbulent region.

less distortion of the wavefront. This approach alone, however, cannot prevent aberrations that arise when a tongue of mixed gas protrudes from the telescope aperture along the axis, which could occur in some wind conditions. In the second approach, a barrier is placed between the two environments. A solid flat exit window (as described above for a helium-filled system) provides the most effective separation, with an air curtain window as an alternative choice.

Air Curtains

Approaches based on air curtains can be considered when a solid exit window is impractical. Air curtains have been widely used as an alternative to solid windows or doors in applications in which one conditioned environment must be separated from another. These applications generally facilitate the passage of people or vehicles and minimize heating or air-conditioning losses. A jet of air is blown across the opening, and the momentum of the jet provides a degree of stiffness against wind currents that might otherwise blow through the opening. Commercially available air curtain devices are produced in a wide range of sizes and are typically powered by self-contained electric fans. A single-layer air curtain is installed at the exit of the Sealite beam director shown in Fig. 1.

Single-Layer Air Curtain

Figure 11 illustrates the basic features of an air curtain device as applied to a telescope. A jet of air issues from a rectangular nozzle at moderate speed (typically 10 to 30 m/sec) across the telescope exit aperture. The jet mixes with conditioned air on the inside and with ambient air on the outside, in turbulent layers that increase in thickness across the aperture. Depending on the thickness of the jet, the mixing layers may merge before they reach the far side of the aperture. If the source of the jet flow is ambient air, and is propelled by electric fans that are themselves cooled by the flow, then the static temperature of the emerging jet can be slightly higher (typically less than 0.5 K) than ambient, with the temperature rise attributable to the inefficiency of both the motor and the fan. The temperature of the conditioned air inside the telescope may differ by several degrees from the ambient temperature if, for example, the ambient temperature is changing rapidly. As a result, three intermingling temperature zones exist within the air curtain. These zones can cause significant wavefront distortions of high spatial and temporal frequency.

The statistical properties of these distortions over the full aperture may be inferred from measurements of the optical path length at fixed points within the aperture. The optical path

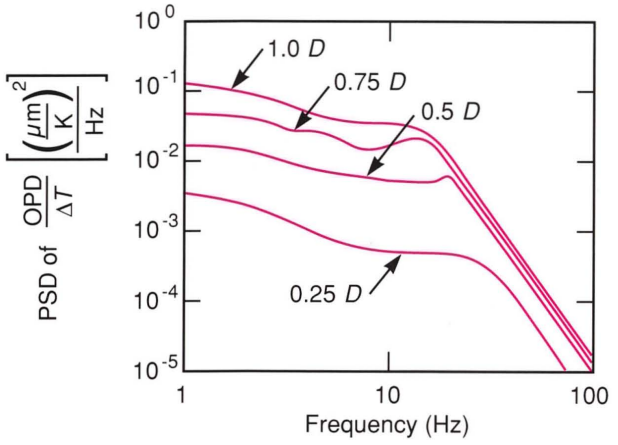

Fig. 12—Temporal spectra of optical path-length difference for a 3.5-m-diameter air curtain normalized to 1 K of temperature difference. Curves are scaled from measured data.

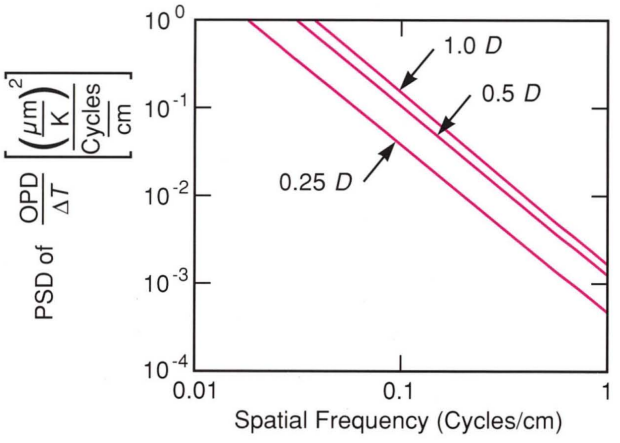

Fig. 13—Spatial spectra of optical path-length difference for a 3.5-m-diameter air curtain normalized to 1 K of temperature difference. Curves are derived from measured data.

length through the curtain is defined as the integral of the refractive index over a fixed distance that includes the jet and mixing zones. For air with small temperature variations, perturbations to this integral are proportional (with negative sign) to the variations in static temperature averaged over the same path. Fast-response temperature (resistance-wire) sensors were developed to measure the recovery temperature averaged over the length of the wire (10 cm and 33 cm). (See the box titled "Experimental Techniques.") Perturbations to the optical path length, at the location of the sensor wire, are then inferred from the voltage fluctuations at the output of the sensor system. These sensors were used with subscale air curtain models (10 cm and 60 cm in diameter) to provide basic data that can be scaled to larger systems.

Figure 12 shows the results of measurements from a single sensor and the 60-cm model, scaled to a 3.5-m-diameter telescope and a nominal air curtain speed of 20 m/sec. The sensor output spectrum was measured, converted to the equivalent rms wavefront-distortion amplitude spectrum, and normalized by the temperature difference between ambient and the telescope environment for several stations across the aperture. For geometrically similar systems, the frequency scale is proportional to the jet speed and inversely proportional to the aperture diameter D, and the spectrum amplitude scales inversely with the jet speed and directly with the square of the aperture diameter.

Multiple sensors with variable spacing measured the correlation of the fluctuations in the length of neighboring optical paths as a function of position within the aperture; this correlation allowed us to estimate uncorrectable errors. Figure 13 shows spatial frequency spectra derived from these measurements for several stations within the aperture, normalized by the temperature offset, and again scaled for a 3.5-m-diameter aperture. The integral of the portion of the spectrum at spatial frequencies greater than the Nyquist frequency (the inverse of twice the actuator spacing), summed over the aperture with the indicated weighting, corresponds to the residual uncorrectable wavefront error attributable to the air curtain.

Dual-Layer Air Curtain

The air curtain device described above consists of a single jet. The major source of aberrations for this device occurs in the mixing zone between air at ambient temperature and air at the temperature of the telescope internal environment. The effective thickness of the mixing zone can be reduced by minimizing the velocity difference between the two bodies of air. Figure 14 shows a dual-layer air curtain concept in which the jet is divided into two adjacent layers flowing at equal speed, but supplied from separate sources, one at ambient temperature and

Experimental Techniques

Wavefront distortions can be measured with direct optical measurement techniques such as interferometry, or with indirect techniques such as cold-wire thermometry. Interferometry measures wavefront distortions by passing a laser beam through the flowfield of interest and then combining the laser beam with an undistorted reference beam. The two beams interfere with each other to create light and dark patterns that form a contour map of the optical path-length differences produced by the disturbing flow. In general, short exposure times are required to avoid blurring of the interference fringes caused by movement. A movie of the interferograms was recorded at Lincoln Laboratory to analyze the flowfield dynamically and to determine the aberrations produced by thermal turbulence present in the wake of a 30-cm thin flat plate. Figure A is one frame of a movie recorded at 2000 fps (500-μsec exposure). Every fourth frame of the movie was analyzed over a 1-sec period to yield the time history of the optical path difference shown in Fig. B. These data were transformed to yield the power spectral density of the optical path difference shown as the red curve in Fig. C.

Several problems arise when interferometry is used to analyze turbulence. One problem is the difficulty in imaging small-scale turbulence. The resolution of the interferograms is governed by the separation between the light and dark fringes; in practice no more than 50 interference fringes can be analyzed. For the 30-cm-diameter aperture shown on the left in Fig. A this limitation translates to a maximum spatial resolution of 6 mm. Another problem is that the interferograms form a contour map of the optical path differences but do not determine sense (positive or negative deviations). The problem is solved by phase-shifting the beam that forms the interference fringes and recording the changes in contour maps. This technique typically requires taking three to five interferograms of the distortion, which is not practical when the distortions change rapidly in time. In addition, the equipment for interferometry can be bulky and expensive. Analyzing the data, particularly the dynamic components, requires a frame-by-frame analysis of a large number of interferograms. Even with automated fringe-following computer programs this procedure can be an extensive undertaking.

Indirect measurement techniques such as resistive-wire thermometry can be used to avoid the problems with interferometry. This method employs a thin wire sensor whose resistance is a calibrated function of temperature. The frequency response of the wire is governed by its thermal time constant, which in turn is easily controlled by making the wire thin so that it heats up and cools down rapidly. Thin wire sensors are commonly used by fluid dynamicists to investigate thermal turbulence. If two or more wires are separated by a known distance, then the correlation function of the turbulence can be determined, which allows the power spectrum of the optical path difference to be determined in spatial frequency (see Fig. 13). Fluid dynamicists are typically interested in the behavior of individual *turbules*; therefore, they try to make the sensors smaller than the smallest scale of the turbulence that they are investigating.

At Lincoln Laboratory the primary interest was in the behavior of several turbules integrated over an optical path length. The standard resistive-wire thermometer was modified by making the sensor long enough to encompass the entire optical thickness of the flowfield in question. The output of the sensor is the instantaneous temperature of the beam path conditioning gas integrated along an optical path (the recovery temperature generally lies between the static and stagnation temperatures—for low speeds, these temperatures are essentially equal). For an incompressible flowfield, this output differs from the optical path difference by the scalar dn/dT.

The modified sensors were made with 3.8-μm-diameter tungsten wire at lengths up to 33 cm. A modified sensor collected data at several points in the aperture, and the curve shown in Fig. C was generated by taking the area-weighted rss of the collected data to generate a curve equivalent to the interferometer data (shown in red).

the other at telescope temperature. The mixing and aberrations now occur in a relatively thin mixing layer that corresponds to the wake of the dividing plate. Measurements were performed on a 60-cm model of a dual-layer curtain by using both the temperature-averaging sensor

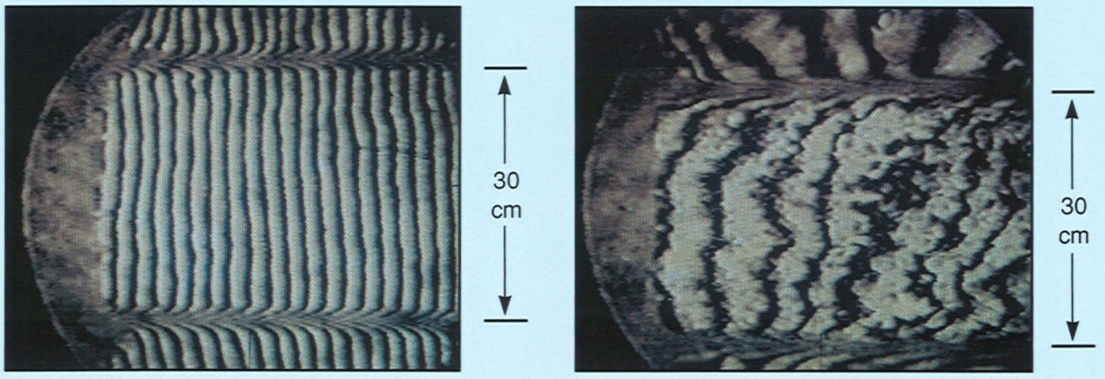

Fig. A—Double-pass interferograms of the thermal turbulence produced by a dual-layer air curtain: (left) a tare interferogram (no flow, no thermal gradient); (right) a 4-m/sec flow with a 16 K temperature difference.

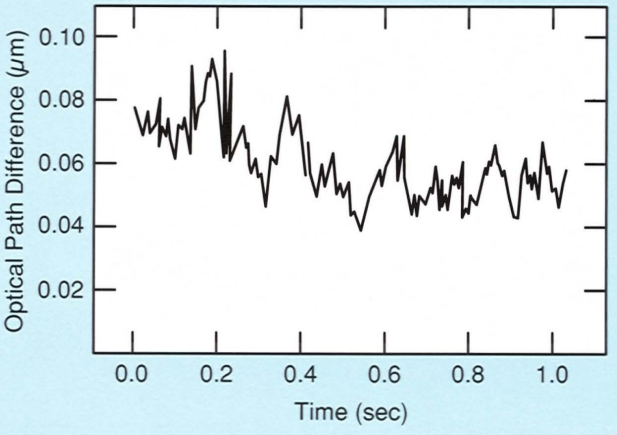

Fig. B—Time history of optical path difference as determined by analyzing 500 consecutive interferograms of the type shown on the right in Fig. A. The exposure time was 500 μsec and the time between frames was 2 msec.

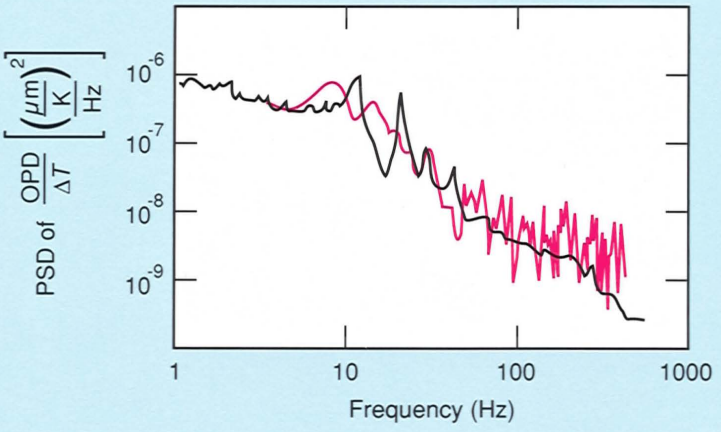

Fig. C—The red curve corresponds to the power spectrum of optical path difference per Kelvin temperature difference, and is determined by transforming the data in Fig. B. The black curve is the rss of the area-weighted measurements of the integrating sensor.

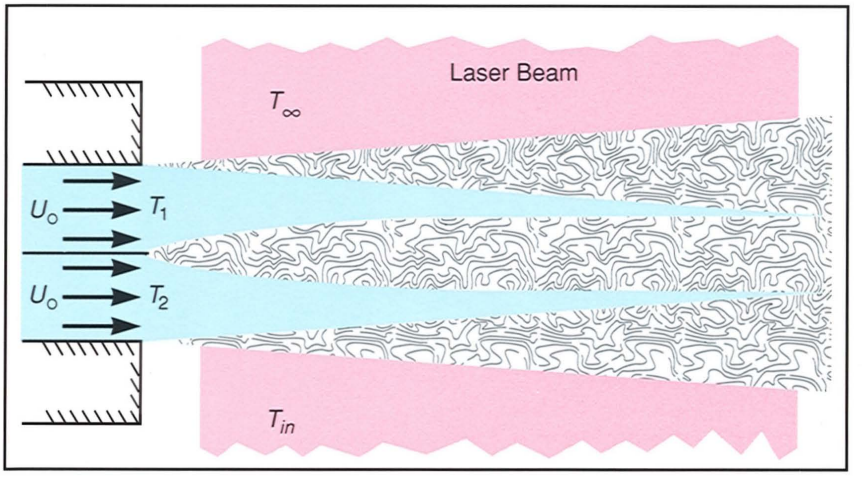

Fig. 14—Dual-layer air curtain. The two jets at temperatures T_1 and T_2 sweep with initial velocity U_0 across the exit aperture, which separates the ambient environment from the beam path conditioning system. This window has improved performance over the single-layer window, but at the cost of additional air-handling equipment. Ideally, $T_1 = T_\infty$, and $T_2 = T_{in}$, which restricts thermal turbulence to the shear-free wake.

and optical interferometry. The residual uncorrectable wavefront error was almost an order of magnitude smaller than that for the single-layer air curtain, for the relatively low jet speeds at which compressibility effects are negligible.

Compressibility Effects

The ability of the air curtain to resist disturbances from wind loading depends on the jet momentum, which is proportional to the product of the overall jet thickness and the square of the jet speed. As we have seen, compressibility introduces an aberration component that is proportional to the square of the jet speed. This behavior favors the use of relatively thick jets. Figure 15 compares the performance of the single-layer and dual-layer air curtains and indicates the effects of compressibility. The performance advantage of the dual-layer air curtain over the single-layer air curtain applies only at relatively low jet speed; at speeds above 20 m/sec compressibility effects for both designs dominate the aberrations. For comparison, the optical path-length differences produced by the thermal boundary layers on a solid exit window are shown. These data indicate that optical distortions can be significantly reduced if a high-quality solid exit window is used.

Entrainment by Air Curtain

The air curtain jet mixes with and entrains air from both inside and outside the telescope, in the manner of an ejector pump. The flow of conditioned air entrained from the telescope

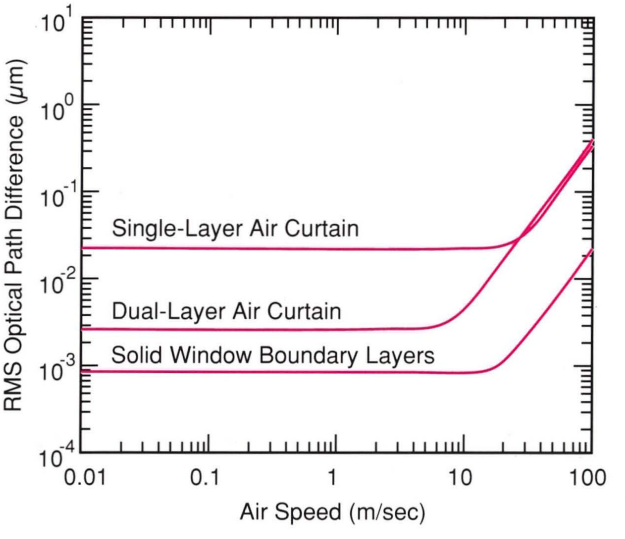

Fig. 15—Relative rms optical path difference for the exit window designs with a 1 K temperature difference and a 1-m-diameter aperture for a single-layer air curtain window, a dual-layer air curtain window, and a solid exit window with radial boundary-layer control jets. The dual-layer air curtain has significantly better optical performance but a slightly higher compressibility penalty. The solid window is the most expensive option but has the best performance.

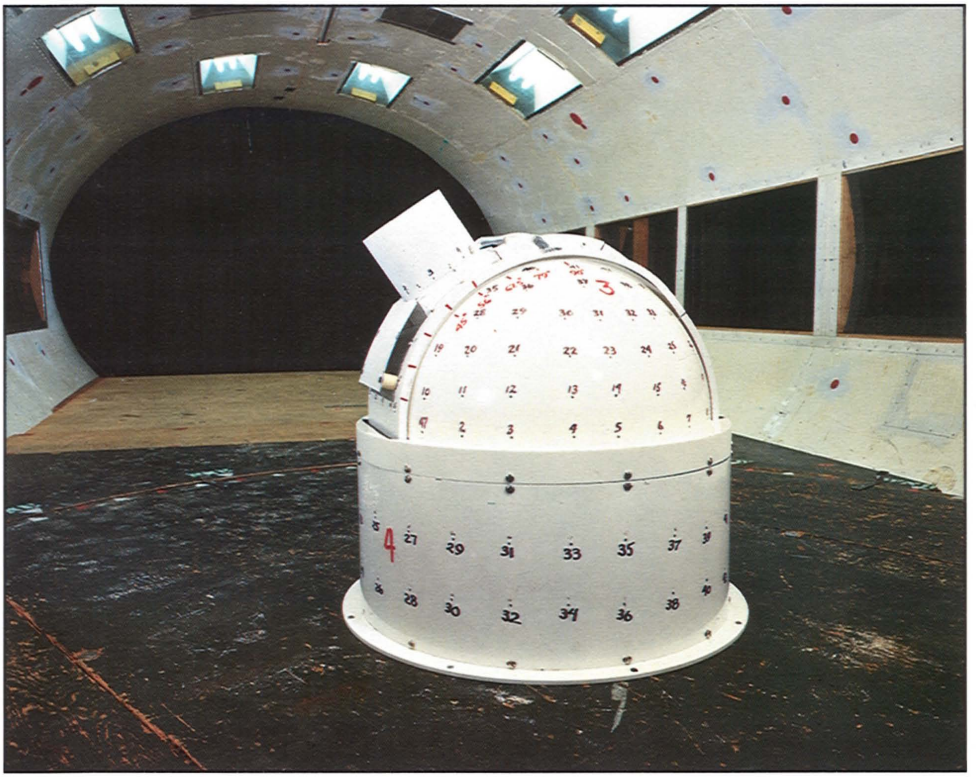

Fig. 16—A 60-cm-diameter dome with mounted air curtain undergoing wind tunnel testing. The circular fence over the exit aperture is designed to prevent mixing of the air curtain and the dome boundary layer.

side must be provided by the telescope ventilation system. If the telescope is enclosed in a tube and this flow is not provided, the pumping action of the curtain jet reduces the pressure in the telescope tube, and the jet deflects inward until a sufficient fraction of the jet is recirculated back into the telescope to bring equilibrium. Large increases in wavefront distortion can be expected in this case, since the inner mixing zone can now include the entire telescope tube. Dynamic instabilities such as organ-pipe oscillations can also occur. The ventilation flow rate is accordingly set by the design of the air curtain (if an air curtain is used).

Wind Loading of Air Curtain

Practical systems are influenced by wind loading of the air curtain, and wind tunnel tests are used to evaluate these effects. Figure 16 shows a 60-cm-diameter scale model of a dome with an air curtain, installed in the MIT Wright Brothers facility. Air curtain behavior is measured with a 10-cm averaging temperature sensor, as a function of wind direction and speed. Figure 17 shows examples of distortion spectra. As the wind speed approaches half the air curtain speed, the curtain begins to oscillate and becomes ineffective as a barrier.

Coudé Path Conditioning

The coudé path (following the terminology of astronomical telescopes) is the system of connecting tubes and relay mirrors required to direct the unexpanded laser beam into the telescope. Ideally, the vacuum window is placed at the entrance to the beam expander; however, this placement may be impractical for some systems, and the conditioning of this portion of the beam path must be controlled.

Thermal sources in the coudé path include the laser energy absorbed directly by the conditioning gas, heat convected from the relay mirrors, and heat convected from the coudé path enclosure (which may be heated by wide-angle

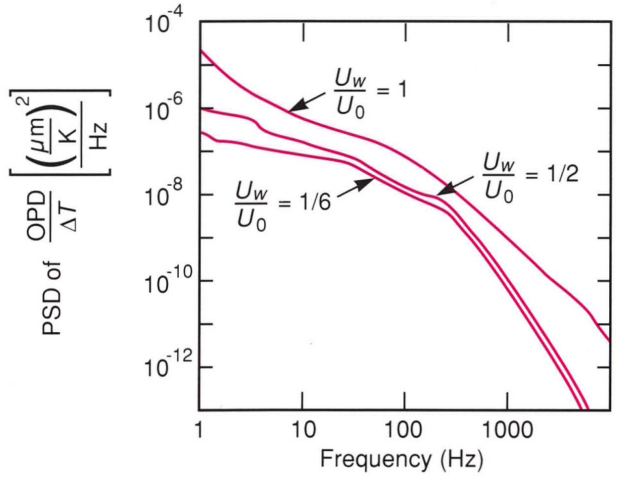

Fig. 17—Spectra of air curtain optical path difference for different ratios of wind velocity to air curtain velocity. Low-frequency fluttering occurs as the wind approaches half of the air curtain speed; this effect can compromise the integrity of the window. The 10-cm air curtain was at zero zenith angle.

scatter from the mirrors). Figure 18 shows the axial-flow approach and the cross-flow approach for coudé path conditioning. Axial flow, shown in Fig. 18(a), relies on turbulent mixing along the beam path to homogenize the temperature gradients. Effective mixing is promoted by the secondary flows that are generated at the elbows (recirculation zones within the ducts must be suppressed). The heat added to the flow is carried through the beam path, and the wall thermal boundary layers enter the beam path, which requires vigorous mixing or boundary-layer suction (Fig. 18[b]) to attenuate these disturbances. Axial flow is the only practical option within the confined beam path through the gimbals of a telescope mount. Figure 18(c) shows a cross-flow beam duct. Here the thermal boundary layers on the duct sidewalls are kept out of the beam path. In this arrangement the upstream gas plenum outlet screen must be shielded from stray laser radiation. Otherwise, hot streams of conditioning gas can flow directly across the beam path.

Beam Director Internal Flow

The flow within a conditioned telescope can be complicated. The use of an exit air curtain

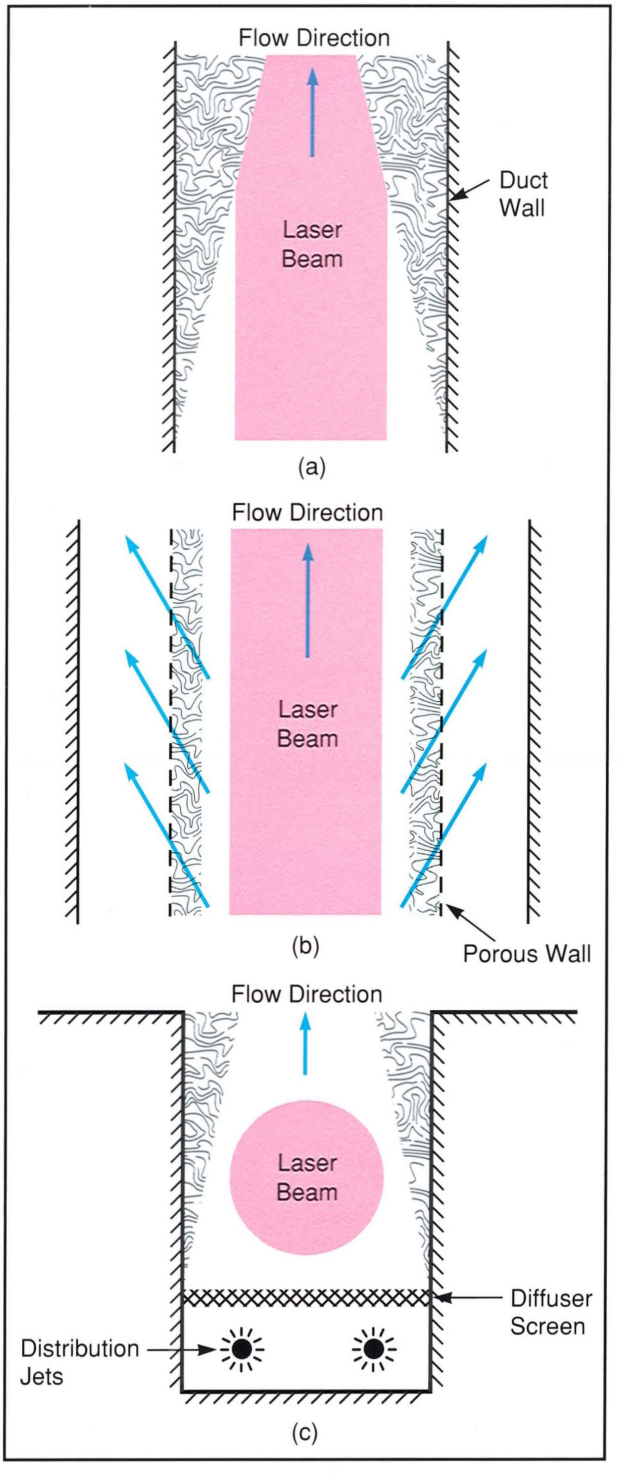

Fig. 18—Beam path conditioning options for coudé path: (a) axial flow allows thermal boundary layers to intrude into the beam path; (b) axial flow with boundary-layer suction is an alternative way to increase control over the beam path gas; (c) transverse flow allows for more control over the air contained in the beam path but requires more air-handling equipment.

requires a substantial makeup flow. This flow is commonly ducted into the telescope via the coudé path; it enters the telescope tube as a jet and induces a number of secondary turbulent flows. These three-dimensional turbulent flow fields are currently studied most easily with subscale physical models. These models show that the inflowing jet scours the thermal boundary layer of the central turning mirror (the Nasmith mirror that redirects the beam toward the secondary mirror); the jet can also produce a reverse flow at the surface of the primary mirror. Recirculation zones become established within the telescope tube and trap cells of overheated air in the beam path. Supplementary jets are added to suppress recirculation and promote mixing. In general, accurate models of the proposed telescope structure and flow apparatus must be built and tested to provide confidence in the design of the conditioning system.

Conclusions

Sources of optical aberration caused by heat-generated density gradients in the gaseous medium can exist in the internal beam path of high-power laser systems. The gradients are reduced by gas flows, but because they also arise from high flow speed, optimum speeds must be found. System designs require the integration of a variety of flowing gas systems that interact with one other. Further development of full-aperture vacuum windows will virtually eliminate these sources of aberration.

Acknowledgements

We would like to acknowledge Glenda S. Holderbaum for her work on the spherical-dome vacuum windows and Darryl E. Weidler for his work on segmented exit windows. Their work contributed greatly to the scope of this paper.

References

1. J.W. Hardy, J.E. Lefebvre, and C.L. Koliopoulos, "Real Time Atmospheric Compensation," *J. Opt. Soc. Am.* **67,** 360 (1977).
2. D.C. Johnson and G.S. Holderbaum, "Beam Path Conditioning for High Energy Beam Directors," *SPIE Proceedings* **1312**, 422 (1990).
3. W.H. Steavenson, "Air Disturbance in Reflectors," *Vistas Astr.* **1,** 473 (1955).
4. E.M. Parmentier and R.A. Greenberg, "Supersonic Flow Aerodynamic Windows for High-Power Lasers," *AIAA Journal* **11,** 943 (1973).
5. G.S. Holderbaum and R.J. Phillips, "Spherical Vacuum-Interface Window with Axial-Flow Impingement Cooling," *SPIE Proceedings* **1047,** 141 (1989).
6. R.B. Dunn, "Sacramento Peak's New Solar Telescope," *Sky and Telescope* **38**, 368 (Dec. 1969).
7. D.E. Weidler, "Large Exit Windows for High Power Beam Directors," *SPIE Proceedings* **1047,** 153 (1989).
8. D.C. Johnson, "Boundary Layer Control for Large Optics," *SPIE Proceedings* **1047,** 174 (1989).

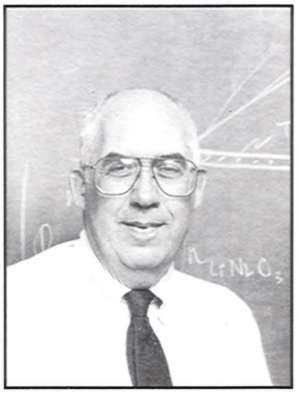

TIMOTHY STEPHENS is a senior staff member in the Optical Systems Engineering Group. He has a Bachelor's degree in Applied Science, Mechanical Engineering, from Queen's University in Kingston, Ontario, and an S.M. in Aeronautics and Astronautics from MIT. His research speciality is in electromechanical systems engineering. Tim has spent 28 years at MIT, and 19 of those years have been at Lincoln Laboratory.

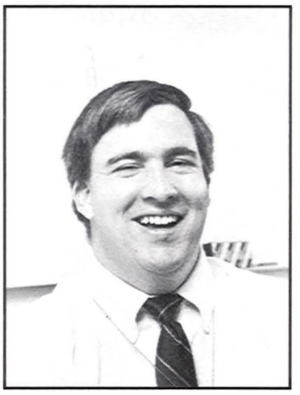

DAVID JOHNSON is an associate staff member in the Optical Systems Engineering Group. His research field is turbulent fluid mechanics. Dave was a sergeant in the U.S. Army Airborne Infantry before attending the University of Illinois, where he received a B.S. in mechanical engineering. He has been at Lincoln Laboratory since 1987.

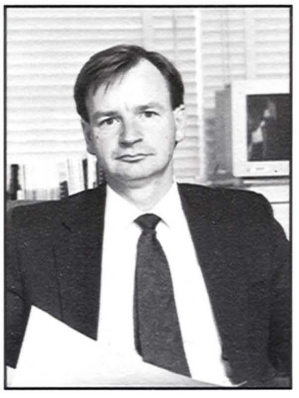

MICHAEL LANGUIRAND is an Assistant Leader in the Optical Systems Engineering Group. His research speciality is mechanical engineering for optical systems. He received a B.S. degree from the University of Lowell, and M.S. and Ph.D. degrees from Rensselaer Polytechnic Institute, all in mechanical engineering.